Journal of Zhejiang University SCIENCE A
ISSN 1673-565X (Print); ISSN 1862-1775 (Online)
www.zju.edu.cn/jzus; www.springerlink.com
E-mail: jzus@zju.edu.cn

Emission and drying kinetics of paper mill sludge during contact drying process*

Wen-yi DENG, Xiao-dong LI†‡, Jian-hua YAN, Fei WANG, Sheng-yong LU, Yong CHI, Ke-fa CEN

(*State Key Laboratory of Clean Energy Utilization, Institute for Thermal Power Engineering, Zhejiang University, Hangzhou 310027, China*)

†E-mail: lixd@zju.edu.cn

Received Sept. 7, 2008; Revision accepted Jan. 8, 2009; Crosschecked Sept. 10, 2009

Abstract: The emission and contact drying kinetics of the paper mill sludge (PMS) were studied through experiments carried out in a paddle dryer. To get a better understanding of its drying mechanism, a penetration model developed by Tsotsas and Schlünder (1986) was used to simulate the drying kinetics of the PMS. The result indicated that this kinetics could be divided into three phases: pasty, lumpy and granular phases, and could be successfully simulated by the penetration model as the related sludge parameters were integrated into the model. The emission rate curves of the volatile compounds (VCs) were interrelated to the drying rate curve of the PMS, especially for volatile fatty acids (VFAs) and ammonia in this study.

Key words: Contact drying, Emission, Paper mill sludge (PMS), Paddle dryer
doi:10.1631/jzus.A0820648 **Document code:** A **CLC number:** X705

INTRODUCTION

The pulp and paper making industry not only consumes a large quantity of water but also generates greatly wastewater. In China, over 374.4×10^6 t of wastewater from pulp and paper making industry are generated each year, which produces about 75×10^3 t of paper mill sludge (PMS). Disposing PMS environment friendly is a big challenge to the paper industry. At present, landfill is the main solution to PMS disposal in China. But with the further constraining of the Chinese legislation on the sludge dumping, in the near future, the sludge dumping on dump sites will be permitted only as its water content is less than 1.5 kg water per kg dry solid (DS).

For either using or disposing sludge, such as agricultural utilizing, incinerating, or landscaping, a low water content of the sludge is usually required (Grüter *et al.*, 1990). Thermal drying is an important intermediate step in the process of all disposal methods, since it helps to stabilize the sludge, to reduce its volume and to abate the odor of the products (Vesilind and Ramsey, 1996). Thermal drying by different dryers has been widely applied to sludge drying process (Chen *et al.*, 2002). In terms of heat and mass transfer, the available dryers can be classified as the indirect dryer, the direct dryer and the combination dryer (Lowe, 1995; Hudson and Lowe, 1996). Comparing with the direct ones, the indirect dryers have the advantages of minimal amount of vapor produced, no pollution of heat carrying medium, lower energy consumption and less operation cost (Ferrasse *et al.*, 2002). Typical indirect dryers are paddle dryer, thin-film dryer and rotary-disc dryer. What we are focusing on here is the contact drying technologies with agitators (the paddle dryer).

The design of sludge dryer and the determination of its operation parameters require knowledge of the drying kinetics, which strongly depends on the sludge origin. A mathematical model for drying kinetics makes it possible to simulate the process and simplifies the calculation of its design. With respect to the contact drying, Schlünder and Mollekopf (1984) developed a penetration model to simulate the vacuum

‡ Corresponding author
* Project (No. 2007C03003) supported by the Key Project of Science and Technology of Zhejiang Province, China

contact drying of mechanically agitated particulate materials. In this model, the continuous mixing process is replaced by a sequence of contact periods of length t_R, and the model postulates that the contact drying is a purely heat transfer controlled process with two heat transfer resistances, i.e., the contact resistance and the penetration resistance. Dittler *et al.*(1997) extended the model to simulate the contact drying of a pasty material. A few years later, the penetration model was successfully extended by Arlabosse and Chitu (2007) to simulate the contact drying of sewage sludge.

In this study, the contact drying kinetics of the PMS in the presence of air was experimentally studied and simulated based on the penetration model. The emission control of odor-causing volatile compounds is also important during a sludge drying process, and requires knowledge of the emission characteristics of volatile compounds (VCs). Our previous study (Deng *et al.*, 2008) identified the main VCs emissions during the PMS drying process conducted in a tubular furnace and a pilot-scale paddle dryer. In this study, the emission characteristics of the VCs were further investigated.

MATERIALS AND METHODS

Sludge sample

As shown in Fig.1, a kind of mechanically dewatered PMS with water content of 3.3 kg water per kg DS was used. The PMS was sampled from a paper making factory in Pinghu city of Zhejiang province, China. This kind of sludge was produced from aeration basins of anaerobic/oxic (A/O) wastewater treating system. The components of the PMS were analyzed based on Chinese Standard GB/T 212-2001 (2001) for proximate analysis and GB/T 476-2001 (2001) for ultimate analysis. The results of the proximate and ultimate analysis of the PMS are given in Table 1.

Experimental set up and apparatus

Fig.2 shows the experimental setup of the sludge drying system, which mainly consists of a twin shafts paddle dryer, a condenser and an extraction pump. The paddle dryer is constructed with 16 wedge-shaped paddles and 2 hollow shafts. The diameter

Fig.1 Sludge from paper making factory

Table 1 Proximate and ultimate analysis of PMS (dry basis) (mass fraction)

Component (%)	Value	Component (%)	Value
Ash content	49.73	N	1.07
Volatile content	42.37	S	1.66
Fixed carbon content	3.94	O	23.00
C	16.94	Cl	0.092
H	3.64		

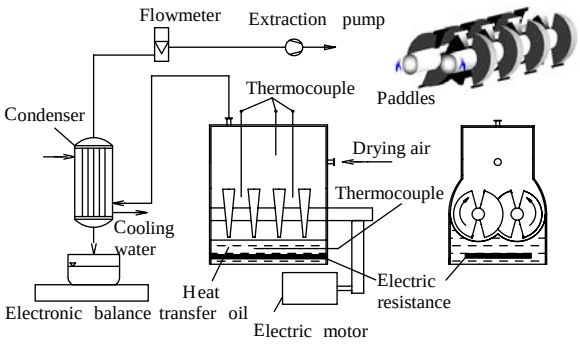

Fig.2 Paddle dryer setup

is 60 mm for the paddles and 25 mm for the shafts. The effective volume of the dryer is 1.1 L, and the dryer was run batch-wise with handling capacity of 1.0 kg wet sludge per batch. The paddles and shafts as well as the jacket of the shell walls were filled with thermal oil that was heated by electrical resistances during the sludge drying process. The temperature in the shafts and jacket was measured by thermocouples. The heating power of the electrical resistance was automatically controlled by a temperature controller to keep the drying temperature stable at the set point. The sludge temperature was measured at two axial positions 1 cm into the product by two different thermocouples. The torque at the stirrer was measured by a torque dynamometer.

As shown in Fig.2, there is an opening for dry air so the sludge drying took place in the presence of air under normal pressure. In the PMS drying experiment, a fixed amount of wet PMS cake (0.941 kg) was fed to the dryer. Water evaporated during the drying process was extracted by an extraction pump, and was introduced to a water-cooled condenser to be condensed and discharged. The drying rate was determined by measuring the condensate mass continuously over the time of the experiment.

Gaseous samples emitted from the PMS drying were introduced into a gas analyzer (Gasmet DX-4000, Finland), which consists of two units: the sampling unit for gases sampling and cleaning; the measuring unit for continuous analysis with Fourier transform infrared (FTIR). The gaseous samples were continuously and automatically measured by the FTIR analyzer, and infra-red spectra obtained were automatically processed by Calcmet Software 2005.

RESULTS AND DISCUSSION

Drying kinetics

The drying experiment was conducted under the temperature (T_{oil}) of 180 °C and stirrer speed (n) of 17 r/min. The results (Fig.3) indicate that the drying process of the PMS in the paddle dryer can be separated into three phases: pasty, lumpy and granular phases, based on the drying rate curve. In the pasty phase, there is a sharp increase in drying rate and then followed by a marked decrease from the peak value. In the lumpy phase, there is a constant drying rate stage which located in the range of the water content between 1.53 and 1.11 kg water per kg DS, and an increasing drying rate stage which was accompanied with a strong increase in torque. The strong increase in torque indicates that the lumpy sludge bulk begins to break up. At the end of the lumpy phase, the torque sharply decreases and the transition towards the granular phase beginning. In the granular phase, the sludge drying rate continuously decreases from the peak value. The torque in this phase is almost negligible compared with the other two phases.

The heat flux density on the heating surface of the paddle dryer can be calculated by the heating power of the electrical resistance (Fig.4). It is obvious that the heat flux density is in direct proportion to the drying rate, thus the drying kinetics of the PMS can also be illustrated by the heat flux density.

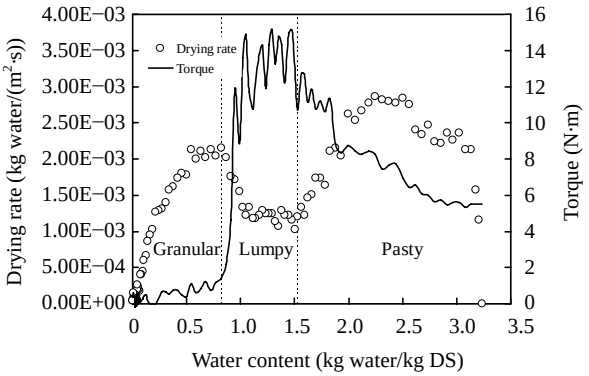

Fig.3 Drying kinetics of the PMS (T_{oil}=180 °C, n=17 r/min)

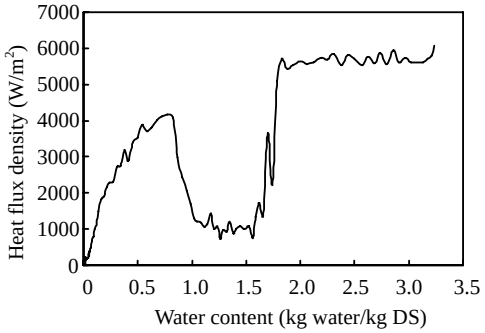

Fig.4 Heat flux density on the heating surface (T_{oil}=180 °C, n=17 r/min)

Contact drying modeling

To further understand the contact drying kinetics of the PMS in the presence of air, a penetration model developed by Tsotsas and Schlünder (1986) was adopted. This model was first used to analyze the contact drying of agitated granular materials in the presence of inert gas, and was extended to model the contact drying of porous hygroscopic materials by Gevaudan and Andrieu (1991). In this model, the steady state mixing process is replaced by a sequence of unsteady mixing steps; a contact period of length t_R is followed by an instantaneous perfect macro-mixing of the bulk; during the contact period, the bulk is assumed to rest on the heating plate to be heated by conduction. The contact resistance between the hot surface of the dryer and the bed, the penetration resistance of the bed, and the mass transfer resistance on the bed surface are the drying rate controlling factors in this model.

Fig.5 shows the temperature profiles and heat fluxes during a contact period, where q_{in}, q_{sen}, q_{out}, q_{lat}, q_{loss} are the heat fluxes from the thermal oil to the PMS bed, the heat flux changing the PMS temperature, the heat flux leaving the bed, the latent heat, and the heat loss, respectively. These heat fluxes can be calculated by the following equations:

$$q_{in} = h_{ws}^{*}(T_{oil} - T_{bed,i}), \tag{1}$$

$$q_{out} = h_{b,w}(T_{bed,i} - T_s), \tag{2}$$

$$q_{loss} = (h_c + h_{rad})(T_s - T_G), \tag{3}$$

$$q_{sen} = (\rho c_p)_{b,w} L \frac{(T_{bed,i+1} - T_i)}{t_R}, \tag{4}$$

$$q_{lat} = \dot{m}_V \Delta H_T,$$

where T_{oil}, T_s, T_G, $T_{bed,i}$ and $T_{bed,i+1}$ are the temperatures of the thermal oil, the bed surface, the ambient air, the bed at the beginning of the contact period, and the bed at the end of the contact period, respectively. h_c is the convective heat transfer coefficient, $\dot{m}_V$ is the drying rate of the PMS, ΔH_T is the total heat of vaporization, L is the height of the sludge bed. $\rho_{b,w}$ and $c_{pb,w}$ are the density and the specific heat capacity of the sludge bed, respectively. h_{ws}^{*} is the heat transfer coefficient from the thermal oil to the first particle layer, and is given by

$$\frac{1}{h_{ws}^{*}} = \frac{1}{h_{oil}} + \frac{1}{h_{wall}} + \frac{1}{h_{ws}}, \tag{5}$$

where the heat transfer coefficient h_{oil} was 445 W/(m^2·°C). The contact surface resistance ($1/h_{wall}$) can be calculated with the thermal conductivity of the wall material and its thickness. $1/h_{ws}$ is the contact resistance between the wall and the first layer of particles, and h_{ws} was calculated to be 174.2 W/(m^2·°C) based on the method introduced by Schlünder and Mollekopf (1984).

The time-averaged heat transfer coefficient for the bulk penetration, $h_{b,w}$ is expressed as

$$h_{b,w} = 2\sqrt{\frac{(\rho\lambda c_p)_{b,w}}{\pi t_R}} = \frac{2\lambda_{b,w}}{\sqrt{K_b \pi t_R}}, \tag{6}$$

where $\lambda_{b,w}$ and K_b are respectively the effective thermal conductivity and thermal diffusivity of the PMS bed.

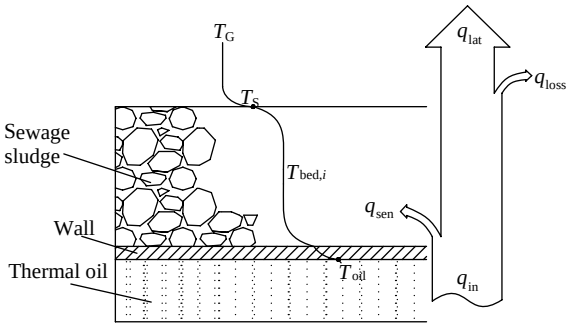

Fig.5 Temperature profiles and heat fluxes during a contact period

ΔH_T is calculated by adding the desorption heat ΔH_{des} to the latent heat of vaporization ΔH_V as

$$\Delta H_T = \Delta H_V + \Delta H_{des}. \tag{7}$$

ΔH_T is the parameter bound to the PMS, and was experimentally determined. A fast transient method based on thermogravimetric analyzers-differential scanning calorimeters (TG-DSC) was elaborated and tested by Ferrasse and Lecomte (2004) for total heat of evaporation ΔH_T determination. In this study, ΔH_T of the PMS was measured based on a TG-DSC (SDT Q600, TA, USA). Fig.6a shows the total heat of vaporization of the PMS.

The moisture content of the bed at the end of the observed contact period X_{i+1} is given by

$$X_{i+1} = X_i - \frac{\dot{m}_V t_R A}{m_{DS}}, \tag{8}$$

where A is the hot surface area of the dryer, and was calculated to be 0.09 m^2. m_{DS} is the dry solid content of the PMS. The contact time t_R is expressed by

$$t_R = N_{mix}/n, \tag{9}$$

where n is the stirrer speed of the shafts. N_{mix} is the mixing number which is usually predicted by existing correlations between N_{mix} and Froude number or by fitting to experimental data (Schlünder and Mollekopf, 1984). Unfortunately, the existing correlations developed by Mollekopf (1983) did not refer to the twin

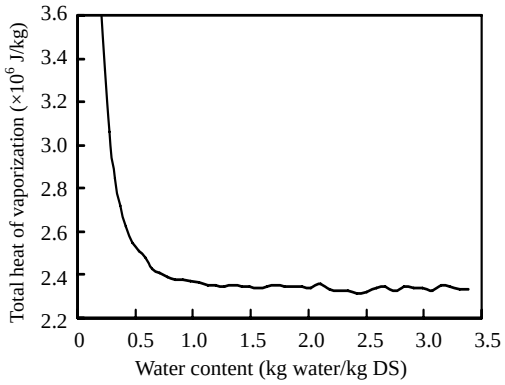

Fig.6 Total heat of vaporization (a) and desorption isotherm (b) of the PMS measured at 90 °C

shafts paddle dryers adopted in this study. As a consequence, the mixing number was determined by fitting to the experimental data.

The drying rate ($\dot{m}_V$) at the PMS bed surface is given by assuming the Lewis hypothesis as

$$\dot{m}_V = \frac{h_c}{c_{P,G}} \frac{M_{H_2O}}{M_{air}} \ln[(P_T - P_V)/(P_T - P_{V,S}(T_S))], \quad (10)$$

where h_c is given by equations (Tsotsas and Schlünder, 1986) that are valid for free and/or forced convection around solid bodies; $c_{P,G}$ is the heat capacity of the carrier gas; M_{H_2O} and M_{air} is the molar mass of water and air, respectively; P_T is the total pressure on the PMS bed surface. The PMS hygroscopicity is taken into account. Therefore, the partial pressure of water vapor ($P_{V,S}(T_S)$) at the bed surface is calculated by modifying the water saturation pressure $P_{V,sat}$ by introducing the water activity (a_w) of the PMS (Gevaudan and Andrieu, 1991):

$$P_{V,S}(T_S) = P_{V,sat} \cdot a_w. \quad (11)$$

a_w was also measured by TG-DSC which was introduced by Ferrasse and Lecomte (2004), and the result is shown in Fig.6b.

Other parameters bound to the PMS are sludge particle diameter (d), thermal conductivity ($\lambda_{b,w}$) and thermal diffusivity (K_b) of the sludge bed, which are important for the contact resistance and penetration resistance calculation. Fig.7a shows the sludge particle diameters in the granular and pasty phases which were determined by a particle size analyzer (Mastersizer 2000, UK). A method introduced by Dewil *et al.*(2005) is adopted for K_b and $\lambda_{b,w}$ determination, and the result are shown in Fig.7b. It can be found that the thermal conductivity of the PMS is nearly constant as the water content is between 2.0 and 3.3 kg water per kg DS, but continuously decreases when the water content is less than 2.0 kg water per kg DS.

As shown in Fig.3, there was a massive decrease in the drying rate within the moisture range of 0.82~2.25 kg water per kg DS, which was caused by additional heat transfer resistance of sludge wall

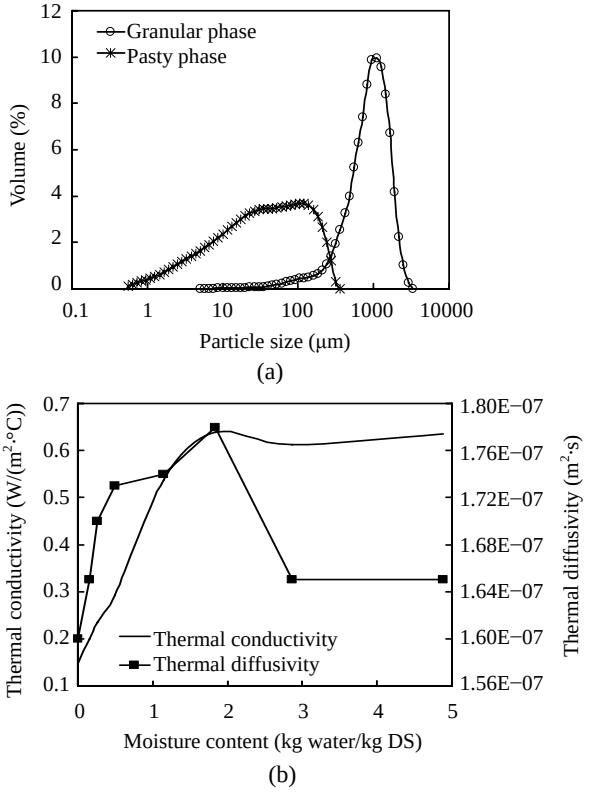

Fig.7 Sludge particle size distributions in the pasty and granular phases (a), and thermal conductivity and thermal diffusivity of the PMS bed measured at 25 °C (b)

formed on the hot surface of the paddles and shafts. According to the drying kinetics discussed above, it is assumed that this sludge wall grows continuously in the moisture range of 1.53~2.25 kg water per kg DS, keeps constant in the moisture range of 1.11~1.53 kg water per kg DS, and decreases continuously in the moisture range of 0.82~1.11 kg water per kg DS. By modifying Eq.(5), this phenomenon can be integrated into the model as

$$\frac{1}{h_{ws}^{*}}=\frac{1}{h_{oil}}+\frac{1}{h_{wall}}+\frac{1}{h_{ws}}+\frac{\delta}{\lambda_{b,w}}. \tag{12}$$

The heat transfer resistance of the sludge wall $\delta/\lambda_{b,w}$ is calculated using a moisture dependent thickness of the sludge wall δ (Fig.8). The maximum thickness of the sludge wall is limited by the depth of the paddles, which is 16.75 mm.

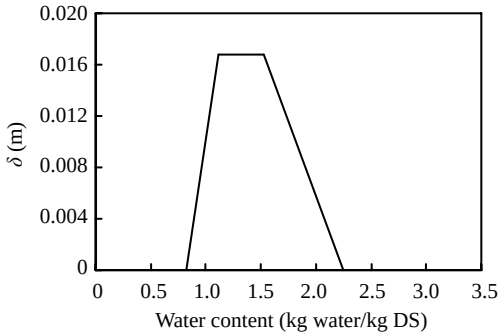

Fig.8 Moisture dependence of sludge wall thickness (T_{oil}=180 °C, n=17 r/min)

Based on the discussion mentioned above, the drying kinetics of the PMS can be calculated theoretically. Fig.9 shows the comparison between the experimental and theoretical data of the drying kinetics. The experimental data and the calculated one are in good agreement, and the heat transfer resistance of the sludge wall can well illustrate the massive decrease in the drying rate in the moisture range of 0.82~2.25 kg water per kg DS. The result also proves that the penetration model can be successfully extended to simulate the contact drying kinetics of the PMS. Fig.9 also shows the comparison between experimental and calculated data of the sludge temperature. The sludge temperature increased quickly from ambient to the experimental temperature at the beginning of the drying process, decreased in the lumpy phase due to deterioration of the agitation

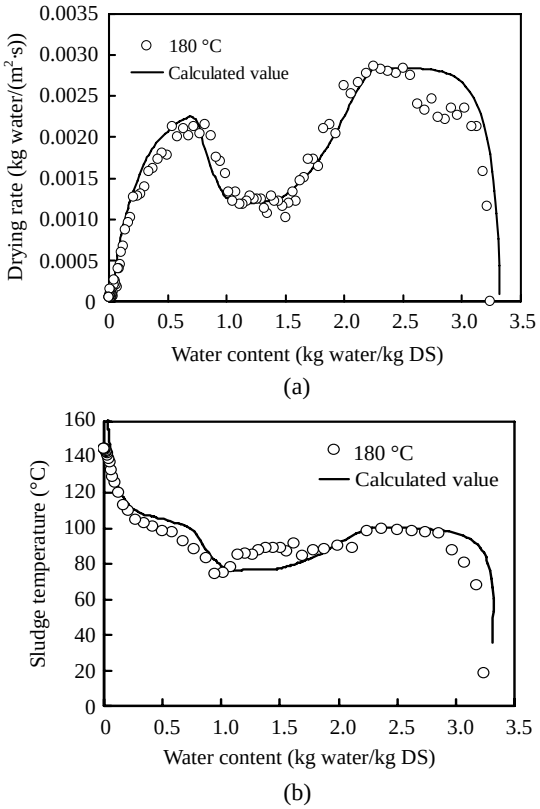

Fig.9 Comparison between experimental (180 °C) and theoretical (calculated value) data of drying kinetics (a) and sludge temperature (b)

effect, and markedly increased in the granular phase. The measured temperature is in acceptable agreement with the calculated temperature.

Volatile compounds emission

Gostelow *et al.*(2001) reviewed odorants measurement and listed 39 typical odorants associated with sewage treatment works, including reduced sulfur bearing compounds, amine compounds, organic acids, aldehydes and ketones. However, the analytical measurements are complicated by the large number of VCs presents, often at concentrations close to the detection limits. It is almost impossible to identify all VCs emissions by one-off measurement. Therefore, the main objectives of this study were to identify the VCs with high concentrations that can be easily identified during the PMS drying process.

The emission characteristics of VCs during the PMS drying process were studied in our previous research (Deng *et al.*, 2008), where the formation mechanisms of VCs were discussed based on the experimental results from a static drying test. The

gaseous samples emitted from sludge drying were continuously measured by an on-line FTIR gas analyzer. The result indicated that mainly five kinds of VCs, i.e., volatile fatty acids (VFAs), heptanes, methane, ammonia and carbon dioxide, emitted during the PMS drying process. Different from previous research (Deng *et al.*, 2008), which focused on the VCs emission from a static drying test and a pilot scale drying test, the evolution of the VCs emission with the decrease of water content during the contact drying process was studied.

In this study, the gaseous sample was continuously measured at the position after the condenser. Fig.10 shows the emission rate of the VCs during the contact drying process. It can be found that the emission rate curves of the VFAs and ammonia (Fig.10) are strongly interrelated with the drying rate curve (Fig.3). The emission abilities of the VFAs, ammonia and heptane markedly decreased in the lumpy phase, where the drying rate of the PMS also markedly decreased. Therefore, it can be concluded that the emission rates of the VCs were significantly affected by the drying rate of the PMS. Fig.10 also shows that, the emission rates of the heptane and methane markedly increased at the end of the PMS drying process. The reason is that, firstly, as shown in Fig.9, there was a sharp increase in sludge temperature at the end of the drying process; secondly, as discussed in our previous research (Deng *et al.*, 2008), the heptane and methane are formed from thermal degradation of more complex organics. As a consequence, the higher temperature will promote the formation of the heptane and methane.

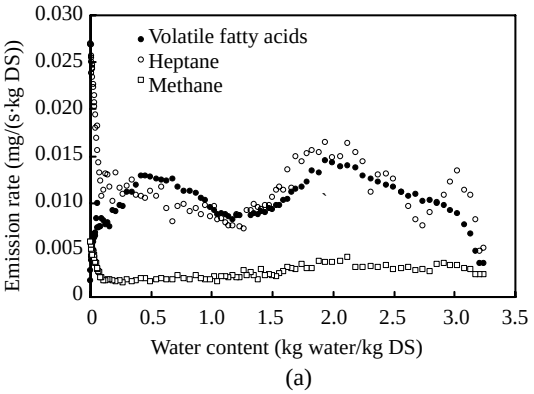

(a)

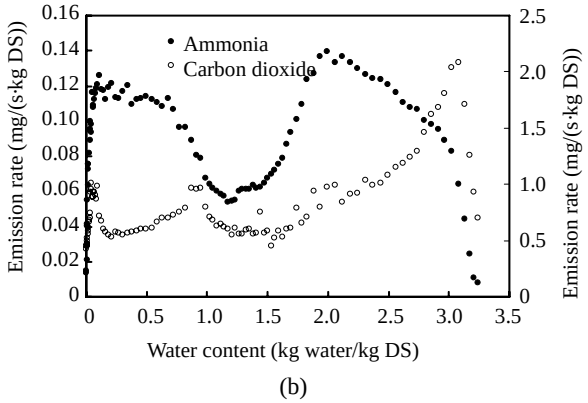

(b)

Fig.10 Emission rates of VAFs, heptane, methane (a), and ammonia, carbon dioxide (b) during the PMS drying process (T_{oil}=180 °C, n=17 r/min)

CONCLUSION

Contact drying kinetics of the PMS in a paddle dryer can be divided into three distinct phases, i.e., pasty, lumpy and granular phases. There was a marked decrease in drying rate in the lumpy phase due to the deterioration of the agitation effect of the paddles. The model proposed by Tsotsas and Schlünder (1986) can be successfully extended to simulate the contact drying of the PMS, by providing the sludge's parameters, i.e., particle size, desorption isotherm, heat of vaporization, thermal conductivity and thermal diffusivity of the PMS. Based on our previous research (Deng *et al.*, 2008), the emission characteristics of VCs, i.e., VFAs, heptane, ammonia, methane, carbon dioxide, were studied during the contact drying process. The result indicated that the emission rate of the VCs is interrelated to the drying rate of the PMS, especially for the VFAs and ammonia.

References

Arlabosse, P., Chitu, T., 2007. Identification of the limiting mechanism in contact drying of agitated sewage sludge. *Drying Technology*, **25**(4):557-567. [doi:10.080/07373930701226955]

Chen, G.H., Yue, P.L., Mujumdar, A.S., 2002. Sludge dewatering and drying. *Drying Technology*, **20**(4-5):883-916. [doi:10.1081/DRT-120003768]

Deng, W.Y., Yan, J.H., Li, X.D., Wang, F., Zhu, X.W., Lu, S.Y., Cen, K.F., 2008. Emission characteristics of volatile compounds during sludges drying process. *Journal of Hazardous Materials*, **153**(1-2):487-492. [doi:10.1016/j.jhazmat.2007.08.080]

Dewil, R., Baeyens, J., Neyens, E., 2005. Fenton peroxidation improves the drying performance of waste activated sludge. *Journal of Hazardous Materials*, **117**(2-3):161-170. [doi:10.1016/j.jhazmat.2004.09.025]

Dittler, A., Bamberger, T., Gehrmann, D., Schlünder, E.U.,

1997. Measurement and simulation of the vacuum contact drying of pastes in a LIST-type kneader drier. *Chemical Engineering and Processing*, **36**(4):301-308. [doi:10.1016/S0255-2701(97)00004-4]

Ferrasse, J.H., Arlabosse, P., Lecomte, D., 2002. Heat, momentum, and mass transfer measurements in indirect agitated sludge dryer. *Drying Technology*, **20**(4-5):749-769. [doi:10.1081/DRT-120003755]

Ferrasse, J.H., Lecomte, D., 2004. Simultaneous heat-flow differential calorimetry and thermogravimetry for fast determination of sorption isotherms and heat of sorption in environmental or food engineering. *Chemical Engineering Science*, **59**(6):1365-1376. [doi:10.1016/j.ces.2004.01.002]

GB/T 212-2001, 2001. Method for Proximate Analysis of Coal. General Administration of Quality Supervision, Inspection and Quarantine of People's Republic of China.

GB/T 476-2001, 2001. Method for Ultimate Analysis of Coal. General Administration of Quality Supervision, Inspection and Quarantine of People's Republic of China.

Gevaudan, A., Andrieu, J., 1991. Contact drying modeling of agitated porous alumina beads. *Chemical Engineering and Processing*, **30**(1):31-37. [doi:10.1016/0255-2701(91)80006-B]

Gostelow, P., Parsons, S.A., Stuetz, R.M., 2001. Odour measurements for sewage treatment works. *Water Research*, **35**(3):579-597. [doi:10.1016/S0043-1354(00)00313-4]

Grüter, H., Matter, M., Oehlmann, K.H., Hicks, M.D., 1990. Drying of sewage sludge—an important step in waste disposal. *Water Science Technology*, **22**(12):57-63.

Hudson, J.A., Lowe, P., 1996. Current technologies for sludge treatment and disposal. *Water and Environment Journal*, **10**(6):436-441. [doi:10.1111/j.1747-6593.1996.tb00077.x]

Lowe, P., 1995. Development in the thermal drying of sewage sludge. *Water and Environment Journal*, **9**(3):306-316. [doi:10.1111/j.1747-6593.1995.tb00944.x]

Mollekopf, N., 1983. Wärmeübertragung an Mechanisch Durchmischtes Schüttgut mit Wärmesenken in Kontaktapparaten. PhD Thesis, University of Karlsruhe, Germany (in German).

Schlünder, E.U., Mollekopf, N., 1984. Vacuum contact drying of free flowing mechanically agitated particulate materials. *Chemical Engineering and Processing*, **18**(2):93-111. [doi:10.1016/0255-2701(84)85012-6]

Tsotsas, E., Schlünder, E.U., 1986. Contact drying of mechanically agitated particulate material in the presence of inert gas. *Chemical Engineering and Processing*, **20**(5):277-285. [doi:10.1016/0255-2701(86)80021-6]

Vesilind, P.A., Ramsey, T.B., 1996. Effect of drying temperature on the fuel value of wastewater sludge. *Waste Management & Research*, **14**(2):189-196. [doi:10.1177/0734242X9601400208]